Spark Anodizing of β-Ti Alloy for Wear Resistant Coating

H. Habazaki*, T. Onodera, K. Fushimi, H. Konno, K. Toyotake[†]

Graduate School of Engineering, Hokkaido University, Sapporo 060-8628, Japan

[†] Shinko Metal Products, Co., Ltd., Kokusaihamamatsucho BLD., 9-18, Kaigan 1-chome, Minato-ku, Tokyo 105-0022, Japan

*Corresponding author: tel&fax: +81-11-706-6575, e-mail address: habazaki@eng.hokudai.ac.jp

Abstract

Spark anodizing of a bcc solid solution Ti-15% V-3% Al-3% Cr-3% Sn alloy has been performed in an alkaline electrolyte containing aluminate and phosphate using dc-biased ac anodizing to form a wear-resistant coating on the alloy. The coating consists mainly of Al_2TiO_5, with rutile and γ-Al_2O_3 being present as minor oxide phases. Depth profiles of the coating, examined by glow discharge optical emission spectroscopy, have revealed that aluminium species, highly enriched in the coating, distribute uniformly in the coating, while phosphorus species, incorporated from the electrolyte, are located mainly in the inner part of the coating near to the coating/alloy interface. The location of the phosphorus species should be associated with porous nature of the coating, allowing access of the electrolyte directly to the inner parts of the coating. The porosity of the coating is reduced by anodizing to high voltages. The marked improvement of the wear resistance by the coating has been demonstrated from a pin-on-disc wear test.

Keywords**;** spark anodizing, wear-resistant coating, β-Ti alloy, Al_2TiO_5

1. Introduction

Titanium alloys are increasingly used in a wide range of industries, including aerospace, automobile, marine, chemical industry and biomedical fields, due to their high strength-to-weight ratio, high corrosion resistance and good biocompatibility. However, the high friction coefficient and poor wear resistance of the titanium alloys limit their applications unless the alloys are coated with wear-resistant materials.

The coating techniques that have so far been employed for titanium alloys are, i) surface oxidation [1-3], ii) physical vapour deposition (PVD) and chemical vapour deposition (CVD) [4, 5] and iii) electroplating [6]. The conventional anodizing, forming amorphous titanium oxide containing anatase, and thermal oxidation, forming rutile, do not provide a surface layer with sufficient wear resistance. PVD and CVD are rather expensive technique. Further, these as well as thermal oxidation may cause mechanical damage on the substrate alloys, due to grain growth and/or formation of titanium-oxygen solid solution during high temperature treatments. Electroplating of hard materials, such as Ni-P alloys, improves the wear resistance, but the formation of well adherent coating on titanium alloys by electroplating is generally difficult.

Recently, spark anodizing, often also referred to as plasma electrolytic oxidation [7], anodic oxidation by spark discharge [8-10], anodic spark deposition [11] and micro-arc oxidation, has been attracted increased attention to improve surface properties, including corrosion, friction and biocompatibility, of titanium alloys [7, 12-29]. Sparking proceeds during anodizing due to dielectric breakdown of the anodic oxide at high voltages. Spark micro-discharge modifies the structure, composition and morphology of the oxide layer; a thick, highly crystalline and melt-quenched high temperature oxide coating is formed by this process. Although the oxide is exposed locally and instantaneously at extremely high temperatures, 10^3-10^4 K [7], the alloy substrate should be kept at low temperatures, not

causing mechanical damage. Thus, spark anodizing is a promising technique to form a wear resistant hard coating on titanium alloys.

Investigations of spark anodizing to improve the wear resistance of titanium alloys have been limited so far almost exclusively on Ti-6Al-4V alloy [13-15, 19, 30-32]. Alkaline electrolytes containing aluminate have been often used to form hard oxide coatings mainly consisting of Al_2TiO_5. To our knowledge, there are no reports on spark anodizing on Ti-15V-3Al-3Cr-3Sn alloy used in the present study. This bcc solid solution titanium alloy possesses better mechanical properties than the Ti-6Al-4V alloy, having potentially wider applications. Here, we reports on the formation of highly wear-resistant coating on this alloy by spark anodizing in an alkaline electrolyte containing aluminate and phosphate. The coating has been characterized using scanning electron microscopy (SEM), electron probe micro-analysis (EPMA), grazing incidence X-ray diffraction (GIXRD), glow discharge optical emission spectroscopy (GDOES), micro-hardness measurement and pin-on-disc wear test.

2. Experimental

A bcc solid solution Ti-15 mass% V-3 mass% Al-3 mass% Cr-3 mass% Sn alloy plate of 15 x 15 x 1 mm size was degreased in acetone ultrasonically prior to spark anodizing. Spark anodizing was carried out in a water-cooled stainless steel bath, which also served as a counter electrode. Dc biased ac voltage was applied to the specimen using a Chroma 61601 programmable ac power source. The voltages were controlled using PC. It was found from our preliminary experiments that high spark density was not sustained simply by applying a constant dc + ac voltage, due to growth of anodic oxide. Thus, the voltages were adjusted to keep an almost constant ac current of 1.5 kA m^{-2} during anodizing up to a maximum peak voltage of 400 V. The electrolyte used was a 0.15 mol dm^{-3} $K_2Al_2O_4$, 0.02 mol dm^{-3} Na_3PO_4,

0.015 mol dm^{-3} NaOH alkaline solution at 293 K.

The thicknesses of the anodic films formed were measured by an eddy current thickness meter (Kett, LH-300C). The phases in the coatings were identified by grazing incidence X-ray diffraction (GIXRD) of an incident X-ray angle of 1° with Cu Kα radiation. The GIXRD patterns were obtained using Rigaku, RINT2000 system. Surfaces and cross-sections of the specimens were observed by a JEOL JSM-5400 scanning electron microscope equipped with Oxford WDX-400 wavelength dispersive X-ray facilities. Further, depth profiling analyses of the anodic films were carried out by glow discharge optical emission spectroscopy (GDOES) using a Jobin-Yvon 5000 RF instrument in an argon atmosphere of 650 Pa by applying RF of 13.56 MHz and power of 30 W. Light emissions at 121.567, 130.217, 396.152, 178.287, 365.350, 311.071, 425.433, 189.989 for hydrogen, oxygen, aluminium, phosphorus, titanium, vanadium, chromium and tin respectively were monitored throughout the analysis with a sampling time of 0.1 s. The signals were detected from an area of approximately 4 mm diameter. Hardness of the coatings, measured using a Fischer Instruments Fischerscope H100VP with a maximum load of 30 mN, was obtained from the analysis of the load-depth curves. For the measurements of the hardness, cross-sections of the coated specimens were used after diamond polishing. Wear-test was performed by a Takachiho TROS-300 pin-on-disc instrument under the condition of a contact area of 200 mm^2, a load of 980 N, a rotating rate of 5 m s^{-1} and duration of 5 h. In addition to the coated specimen, the non-coated Ti alloy and a SUJ2 steel containing 1.0% carbon, 0.2% silicon and 1.5% chromium were also tested for comparison. The disc material used was a SUJ2 steel and the test was carried out in an oil environment at room temperature. Specific wear rate was calculated by assuming the density of the coating to be 3.0 Mg m^{-3}.

3. Results

3.1. Formation of coatings

The change in the maximum peak voltage during anodizing of the titanium alloy is revealed in Fig. 1. Initial approximately linear voltage increase continues up to about 230 V, with a rate of ~1.1 V s^{-1}. Then, the voltage becomes almost constant, since the current density reached the prescribed value of 1.5 kA m^{-2}, followed by gradual increase in the voltage. The later voltage increase proceeds with an enhanced rate, which is associated mainly with the reduced porosity of the anodic film. The anodizing was performed up to the peak voltage of 400 V.

The change in thickness of the coating with the formation peak voltage (Fig. 2) reveals that thickening of the coating occurs mostly below 350 V. No significant increase in the coating thickness above 350 V indicates that the steep voltage rise in the range is not related to the coating thickness. Thickening of the coating is approximately linear with the charge passed during anodizing. Thus, the coating thickens particularly at a low formation voltage region, in which longer anodizing time is required to increase the peak voltage. During anodizing of the alloy, gas, possibly hydrogen and oxygen, has been continuously evolved. Hydrogen should be produced during cathodic cycles and oxygen should be during anodic cycle of the dc-biased ac anodizing.

3.2. Phases in the coatings

The phases in the coatings formed to several peak voltages were examined by GIXRD (Fig. 3). The GIXRD pattern of the coating formed to 230 V, at which sparking has just commenced, reveals intense substrate peaks, indicating the formation of only a thin oxide layer, in agreement with Fig. 2. A very weak peak, probably corresponding to anatase, appears at $2\theta = 25°$. Further, a broad peak around 20-35° suggests that the main oxide is amorphous.

Since this coating is formed mostly without sparking, poorly crystalline oxide is developed as is well known for titanium and its alloys [1].

In contrast, highly crystalline coatings are developed to the formation peak voltages higher than 230 V. The oxide phases found are Al_2TiO_5, rutile and γ-Al_2O_3, the letter two are minor oxides. Although aluminium is contained in the substrate, its content is only 3 mass%. High concentration of aluminium in the coatings should, therefore, be mainly originated from the electrolyte. Rutile decreases, whereas γ-Al_2O_3 increases, with increasing formation voltage. Rutile may convert to Al_2TiO_5 during sparking by the plasma chemical reaction with aluminate in electrolyte and/or γ-Al_2O_3 formed. No substrate peaks are found for the specimens anodized to 250 V and higher voltages, as can be expected from the formation of thick oxide films shown in Fig. 2. No crystalline phases specific to vanadium, chromium, tin and phosphorus species are resolved from GIXRD. These species may be present in amorphous or poorly crystalline phases or form a solid solution with the highly crystalline phases found.

3.3. Morphology of the coatings

The SEM surface images of the coatings produced by anodizing to 230 V revealed typical features of dielectric breakdown, with a number of approximately circular pores of submicrometer sizes (Fig. 4(a)). During anodizing, sparking becomes larger with increasing formation voltage. Associated with such discharge features, pores in the coating enlarge and the coating surface becomes rough up to 300 V (Figs. 4(a-c)). Interestingly, further increase in the formation voltage to 400 V reduces the pore size and the porosity of the coating (Fig. 4(d)).

The inner parts of the coatings produced by anodizing to 250 and 400 V have also been observed after sputtering for 100 s using the GDOES instrument. This sputtering time

corresponds to the depth of approximately 40% of the coatings as shown later in Fig. 8. The inner parts of the coatings (Fig. 5) are also porous. Again, the porosity is largely reduced by anodizing to 400 V, in agreement with the outer surfaces.

The cross-sections of the coated specimens produced by anodizing to 250 and 400 V (Fig. 6) reveal the formation of granular oxide. Finer oxides with apparently stronger particle-particle bonds are developed after anodizing to 400 V. Thus, it is likely that the coatings with improved mechanical properties are produced by anodizing to higher voltages.

3.4. Composition of the coatings

X-ray images of oxygen, titanium, aluminium, phosphorus, vanadium, chromium and tin, in addition to secondary electron images, are shown in Fig. 7 for the cross-section of the coated specimen produced by anodizing to 400 V. Aluminium, mainly incorporated from electrolyte, distributes relatively uniformly throughout the coating. Other alloy constituting elements are also present uniformly in the coating without any particular enrichment and depression at the available resolution. Phosphorus species are incorporated from the electrolyte, being enriched at the inner part of the coating near to the alloy/film interface.

Similar results have been obtained from GDOES depth profiles of the coatings (Fig. 8). Uniform in depth distribution of aluminium species is evident in the coatings produced by anodizing both to 250 and 400 V. From the comparison of intensities of aluminium and titanium during sputtering of the coatings, it is clear that the aluminium content is higher for the coating produced by anodizing to 400 V than to 250 V. The presence of phosphorus species in the inner part of the coating is clearly seen in these depth profiles. Further, hydrogen is present in the alloy beneath the coating. Bulk hydrogen analysis revealed that the hydrogen content in the bulk of the coated specimen was similar to that before anodizing. Thus, it is unlikely that hydrogen embitterment occurs for the coated specimens.

3.5. Mechanical properties of the coated specimens

Micro-hardness of the coating produced by anodizing to 400 V was 5.3 GPa, being higher than that of the alloy substrate (2.9 GPa). Such high micro-hardness was obtained only when anodizing was performed to high voltages close to 400 V. Apparent sintering of the granular coating due to discharge heat as well as reduced porosity may result in the development of hard coatings by spark anodizing.

Table 1 shows results of wear test of the specimen produced by anodizing to 400 V as well as the non-coated specimen and a wear-resistant SUJ2 steel. Poor wear resistance of the non-coated titanium alloy is evident from the large specific wear rate. Marked reduction of the specific wear rate by the coating is evident, with the rate even lower than that of the wear resistant SUJ2 steel.

4. Discussion

From the present investigations, it has been found that highly wear-resistant coatings can be produced by spark anodizing of Ti-15 mass% V-3 mass% Al-3 mass% Cr-3 mass% Sn alloy. The coatings consist mainly of an Al_2TiO_5 phase, with minor oxide phases of γ-Al_2O_3 and rutile, as in the coatings formed on the Ti-6 mass% Al-4 mass% V alloy in aluminate-containing electrolytes [20]. The highly wear-resistant coatings are produced by anodizing to a high peak voltage of ~400 V. Such high voltage is required to reduce the porosity of the coating, to increase the aluminium content in the coating, and hence to enhance the micro-hardness. The enhanced incorporation of aluminium species, mainly from the electrolyte, at high voltages results in the increase in γ-Al_2O_3 phase. The presence of a three phase mixture of Al_2TiO_5, rutile and alumina in the coating formed on Ti-6Al-4V alloy was explained by eutectic reactions involving decomposition of Al_2TiO_5 into rutile and

alumina [20]. This should not be, however, in the present case since the eutectic reactions must induce the formation of stable α-Al_2O_3 [33], not γ-Al_2O_3 found in the present study. Precipitation of alumina and/or aluminium hydroxide occurs mainly in the pores formed by sparking, while titania should be developed predominantly at the alloy/film interface, owing to the inward migration of oxygen in crystalline oxide under the high electric field [34]. Plasma thermochemical reactions result in the formation of Al_2TiO_5, but heterogeneous distribution of titanium and aluminium species in the coating may contribute to the formation of rutile and γ-Al_2O_3. The actual heterogeneous distribution of both species are not resolved in the present study due to the low spatial resolutions of the analytical tools used. This is a subject of future study.

The surface morphology of the coatings produced by spark anodizing (Fig. 4) is typical of dielectric breakdown of anodic films. Discharge channels are developed in the anodic oxide films. High temperatures, 10^3-10^4 K, and high pressures, 10^2-10^3 MPa, inside discharge channels assist incorporation of electrolyte ions into the coating, plasma thermochemical reactions and deposition of melt-quenched oxides [7]. Thus, the coating with high aluminium content is developed as a consequence of incorporation of aluminium species from the electrolyte. Heat, induced by electron avalanches at the discharge channel [35], induces the formation of an Al_2TiO_5 phase, which is generally formed at high temperatures, and also assists the precipitation of aluminium species. With increasing formation voltage, larger sparks are developed, with discharge pores also enlarged up to 300 V (Fig. 4). Further increase in the formation voltage reduces the porosity, probably associated with enhanced precipitation of aluminium species. The precipitated species fill the pores such that only small pores are found in the coating formed to 400 V.

Phosphorus species are also incorporated into the coating from the electrolyte, but their depth distribution is different from that of aluminium species; aluminium species are

distributed almost uniformly throughout the coating, while phosphorus species are present mainly in the inner part of the coating. In the non-porous, compact anodic films, with amorphous structure, formed on titanium and its alloys by conventional anodizing without sparking, electrolyte species are incorporated into the outer part of the film [36, 37]. In growing amorphous anodic oxide, phosphorus species migrates inwards under a high electric field, probably due to their presence as anionic species, such as PO_4^{3-}. The migration rate of phosphorus species is lower than that of O^{2-} ions, such that the phosphorus species are present only in the outer part of the anodic film. The location of phosphorus species mainly in the inner part of the present coating indicates the access of the electrolyte directly in the inner parts of the coating possibly through breakdown channels. During sparking, new coating materials are developed near the coating surface, within the coating and near the alloy [38]. The results suggest that incorporation of phosphorus species is significant only in the inner parts of the coating. Phosphate anions, in addition to aluminate anions, are incorporated into the discharge channels under a high electric field. Precipitation of aluminium species, assisted by plasma chemical reactions occurs readily in the channel, while precipitation and re-dissolution of phosphate may occurs in the channel owing to relatively high solubility of phosphate salts in alkaline solutions. Thus, further migration of phosphate into the inner parts of the coating proceeds in the channel. Consequently, the concentration of phosphorus species becomes high at the inner parts of the coating near to the alloy/coating interface. However, further detailed studies are required for a better understanding of the depth profiles of the phosphorus species.

5. Conclusions

Hard coatings with superior wear resistance are developed on a β-Ti alloy of Ti-15 mass% V-3 mass% Al-3 mass% Cr-3 mass% Sn by spark anodizing in an alkaline

aluminate-phosphate electrolyte at 293 K. Anodizing to high voltages is a requisite condition to get a coating with low porosity and high hardness. The coating consists of an Al_2TiO_5 phase with minor rutile and γ-Al_2O_3 phases. Aluminium species are incorporated largely from the electrolyte due to plasma thermochemical reactions in discharge channels. Phosphorus species incorporated are mainly located in the inner part of the coating, in contrast to the relatively uniform depth distribution of aluminium species in the coating. The coating improves remarkably the wear resistance of the titanium alloy, and the specific wear rate of the coating is even lower than that of a wear-resistant steel.

Acknowledgments

The present work was supported in part by a Grant-in-Aid for Scientific Research, No. 16360353 from the Japan Society for the Promotion of Science.

References

[1] A. Aladjem, J. Mater. Sci. 8 (1973) 688.

[2] A. Bloyce, P.Y. Qi, H. Dong, T. Bell, Surf. Coat. Technol. 107 (1998) 125.

[3] R.W. Schutz, L.C. Covington, Corrosion 37 (1981) 585.

[4] K.A. Gruss, R.F. Davis, Surf. Coat. Technol. 114 (1999) 156.

[5] T. Grogler, E. Zeiler, A. Franz, O. Plewa, S.M. Rosiwal, R.F. Singer, Surf. Coat. Technol. 112 (1999) 129.

[6] T. Nakayama, J. Katoh, W. Urushihara, Y. Terada, K. Iwai, R&D, Research and Development (Kobe Steel Ltd.) 47 (1997) 65.

[7] A.L. Yerokhin, X. Nie, A. Leyland, A. Matthews, S.J. Dowey, Surf. Coat. Technol. 122 (1999) 73.

[8] P. Kurze, W. Krysmann, H.G. Schneider, Cryst. Res. Technol. 21 (1986) 1603.

[9] W. Krysmann, P. Kurze, K.H. Dittrich, H.G. Schneider, Cryst. Res. Technol. 19 (1984) 973.

[10] K.H. Dittrich, W. Krysmann, P. Kurze, H.G. Schneider, Cryst. Res. Technol. 19 (1984) 93.

[11] G.P. Wirtz, S.D. Brown, W.M. Kriven, Mater. Manufacturing Processes 6 (1991) 87.

[12] T.H. Teh, A. Berkani, S. Mato, P. Skeldon, G.E. Thompson, H. Habazaki, K. Shimizu, Corros. Sci. 45 (2003) 2757.

[13] Y.M. Wang, B.L. Jiang, L.X. Guo, T.C. Lei, Mater. Sci. Technol. 20 (2004) 1590.

[14] Y.M. Wang, D.C. Jia, L.X. Guo, T.Q. Lei, B.L. Jiang, Mater. Chem. Phys. 90 (2005) 128.

[15] X.T. Sun, Z.H. Jiang, S.G. Xin, Z.P. Yao, Thin Solid Films 471 (2005) 194.

[16] P. Huang, K.W. Xu, Y. Han, Mater. Lett. 59 (2005) 185.

[17] H.H. Wu, X.Y. Lu, B.H. Long, X.Q. Wang, J.B. Wang, Z.S. Jin, Mater. Lett. 59 (2005) 370.

[18] Y.M. Wang, T.Q. Lei, B.L. Jiang, L.X. Guo, Appl. Surf. Sci. 233 (2004) 258.

[19] Y.M. Wang, B.L. Jiang, T.Q. Lei, L.X. Guo, Y.P. Cao, Rare Metal Materials and Engineering 33 (2004) 502.

[20] A.L. Yerokhin, A. Leyland, A. Matthews, Appl. Surf. Sci. 200 (2002) 172.

[21] Y. Han, S.H. Hong, K.W. Xu, Surf. Coat. Technol. 154 (2002) 314.

[22] A.L. Yerokhin, X. Nie, A. Leyland, A. Matthews, Surf. Coat. Technol. 130 (2000) 195.

[23] Y.M. Wang, B.L. Jiang, L.X. Guo, T.Q. Lei, Appl. Surf. Sci. 252 (2006) 2989.

[24] X.T. Sun, Z.H. Jiang, Z.P. Yao, X.L. Zhang, Appl. Surf. Sci. 252 (2005) 441.

[25] F. Liu, Y. Song, F.P. Wang, T. Shimizu, K. Igarashi, L.C. Zhao, J. Biosci. Bioeng. 100 (2005) 100.

[26] F. Liu, F.P. Wang, T. Shimizu, K. Igarashi, L.C. Zhao, Surf. Coat. Technol. 199 (2005) 220.

[27] W.B. Xue, C. Wang, R.Y. Chen, Z.W. Deng, Mater. Lett. 52 (2002) 435.

[28] W.B. Xue, C. Wang, Z.W. Deng, R.Y. Chen, T.H. Zhang, J. Mater. Sci. Tech. 18 (2002) 37.

[29] W. Xue, Z. Deng, H. Ma, R. Chen, T. Zhang, Surface Engineering 17 (2001) 323.

[30] B.G. Guo, J. Liang, J. Tian, H.W. Liu, T. Xu, Rare Metal Mater. Eng. 34 (2005) 1897.

[31] Z.H. Jiang, X.T. Sun, Y.P. Li, F.P. Wang, Y.D. Lu, J. Mater. Sci. Tech. 21 (2005) 281.

[32] Y.M. Wang, T.Q. Lei, B.L. Jiang, Y. Zhou, Rare Metal Mater. Eng. 32 (2003) 1041.

[33] H.J. Seifert, A. Kussmaul, F. Aldinger, J. Alloys Compd. 317-318 (2001) 19.

[34] J.P.S. Pringle, Electroche. Acta 25 (1980) 1420.

[35] A.L. Yerokhin, V.V. Lyubimov, R.V. Ashitkov, Ceram. Int. 24 (1998) 1.

[36] H. Habazaki, K. Shimizu, S. Nagata, P. Skeldon, G.E. Thompson, G.C. Wood, Corros. Sci. 44 (2002) 1047.

[37] H. Habazaki, K. Shimizu, S. Nagata, P. Skeldon, G.E. Thompson, G.C. Wood, J. Electrochem. Soc. 149 (2002) B70.

[38] E. Matykina, F. Monfort, A. Berkani, P. Skeldon, G.E. Thompson, P. Chapon, Philos. Mag. 86 (2006) 49.

Figure captions

Fig. 1 Change in the maximum peak voltage with time of dc biased ac anodizing in 0.15 mol dm^{-3} $K_2Al_2O_4$, 0.02 mol dm^{-3} Na_3PO_4, 0.015 mol dm^{-3} NaOH electrolyte.

Fig. 2 Change in the coating thickness with formation peak voltage. The change in the coating thickness with the electric charge passed during anodizing is also shown.

Fig. 3 GIXRD patterns of the coated specimens anodized to the formation peak voltages of 230, 250, 300 and 400 V.

Fig. 4 Scanning electron micrographs of surfaces of the coatings produced by anodizing to (a) 230, (b) 250, (c) 300 and (d) 400 V.

Fig. 5 Scanning electron micrographs of the coatings after sputtering for 100 s using a GDOES instrument. The coatings were produced by anodizing to (a) 250 V and (b) 400 V.

Fig. 6 Scanning electron micrographs of cross-sections of the coatings produced by anodizing to (a) 250 and 400 V.

Fig. 7 Secondary electron image as well as X-ray images of oxygen, titanium, aluminium, phosphorus, vanadium, chromium and tin for a cross-section of the coating produced by anodizing to 400 V.

Fig. 8 GDOES depth profiles in the coatings produced by anodizing to (a) 250 and (b) 400 V.

Table 1 Results of pin-on-disc wear test of the titanium alloy with and without the coating produced by anodizing to 400 V and a SUJ2 steel.

Specimen	Test period (s)	Wear loss (g m^{-2})	Specific wear rate (mm^3 N m^{-1})
Coated	18000	0.5	3.7×10^{-10}
Non-coated	~300	63	$\sim 9.0 \times 10^{-6}$
SUJ2 steel	18000	4.5	1.3×10^{-9}

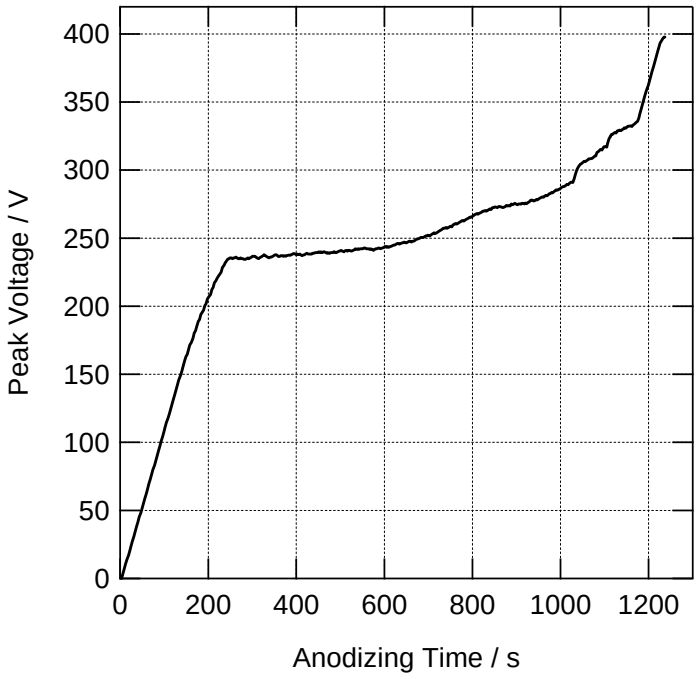
Peak Voltage / V
400
350
300
250
200
150
100
50
0
0
200
400
600
800
1000
1200
Anodizing Time / s

Fig. 1

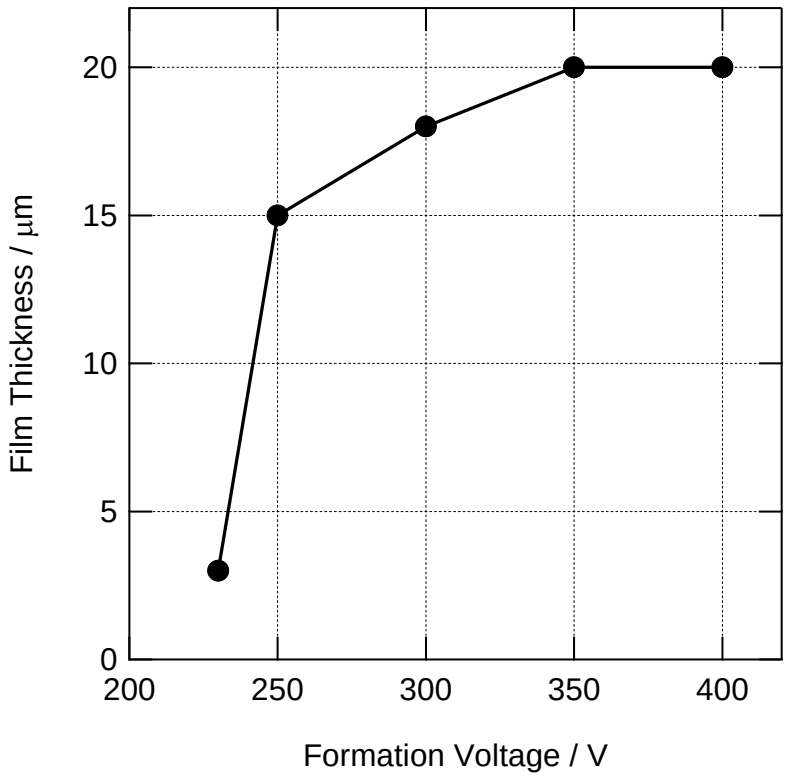
Film Thickness / µm
0
5
10
15
20
200
250
300
350
400
Formation Voltage / V

Fig. 2

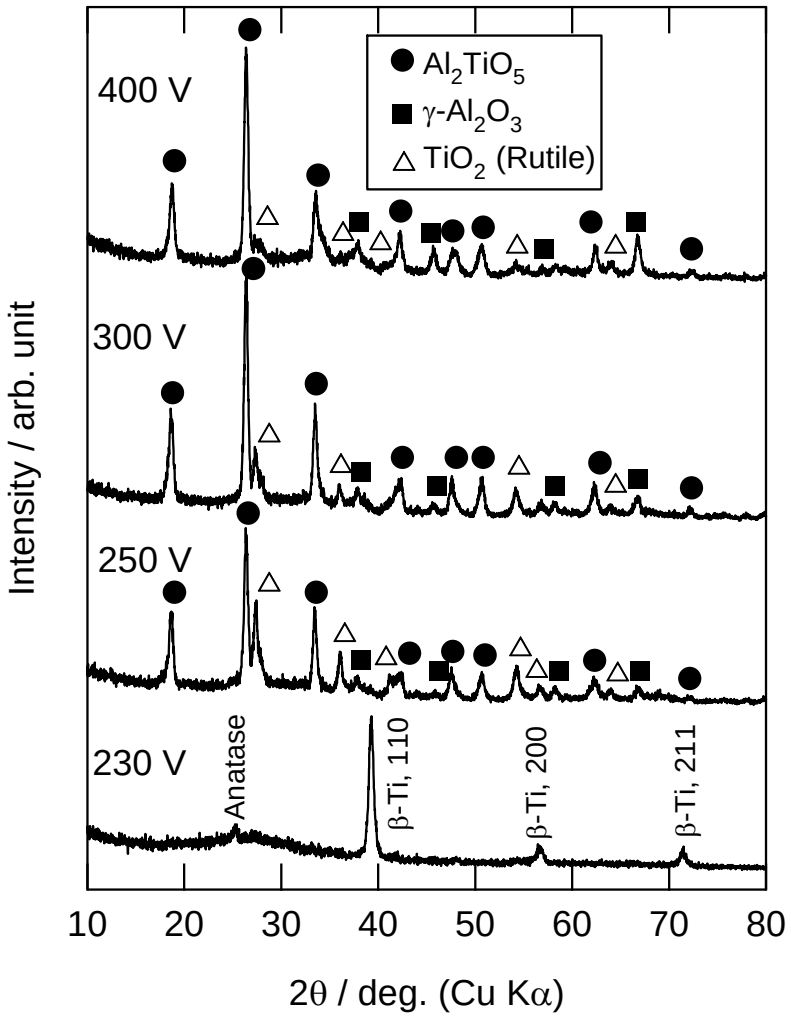
Al2TiO5
γ-Al2O3
TiO2 (Rutile)
400 V
300 V
250 V
230 V
Anatase
β-Ti, 110
β-Ti, 200
β-Ti, 211
Intensity / arb. unit
10
20
30
40
50
60
70
80
2θ / deg. (Cu Kα)

Fig. 3

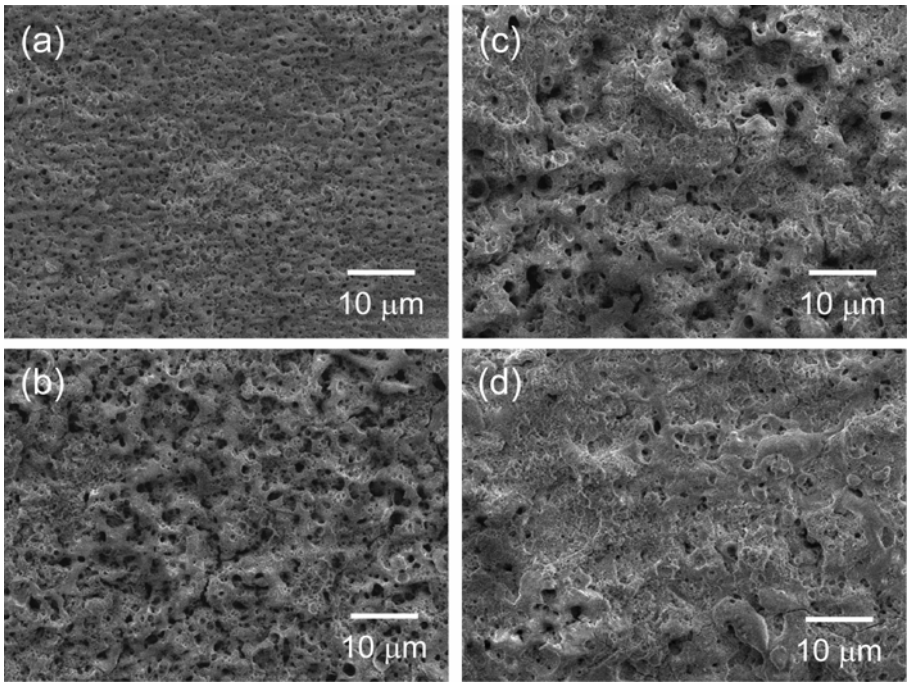

Fig. 4

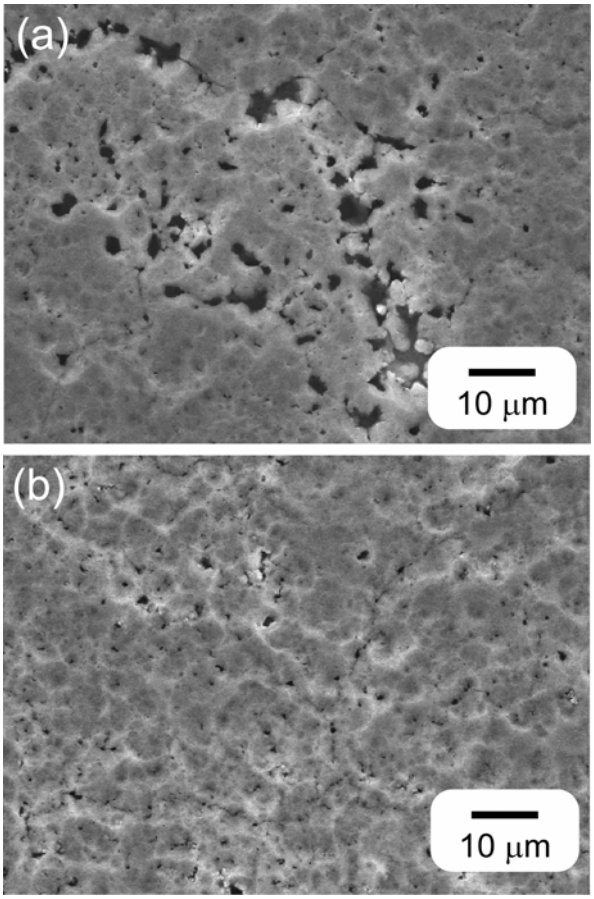

Fig. 5

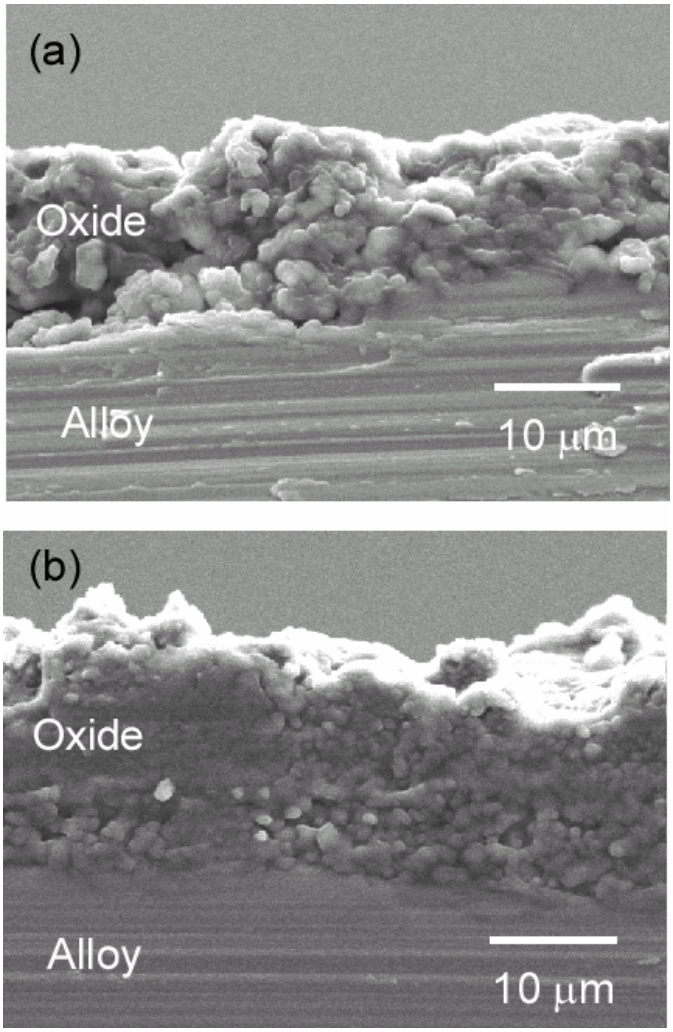

Fig. 6

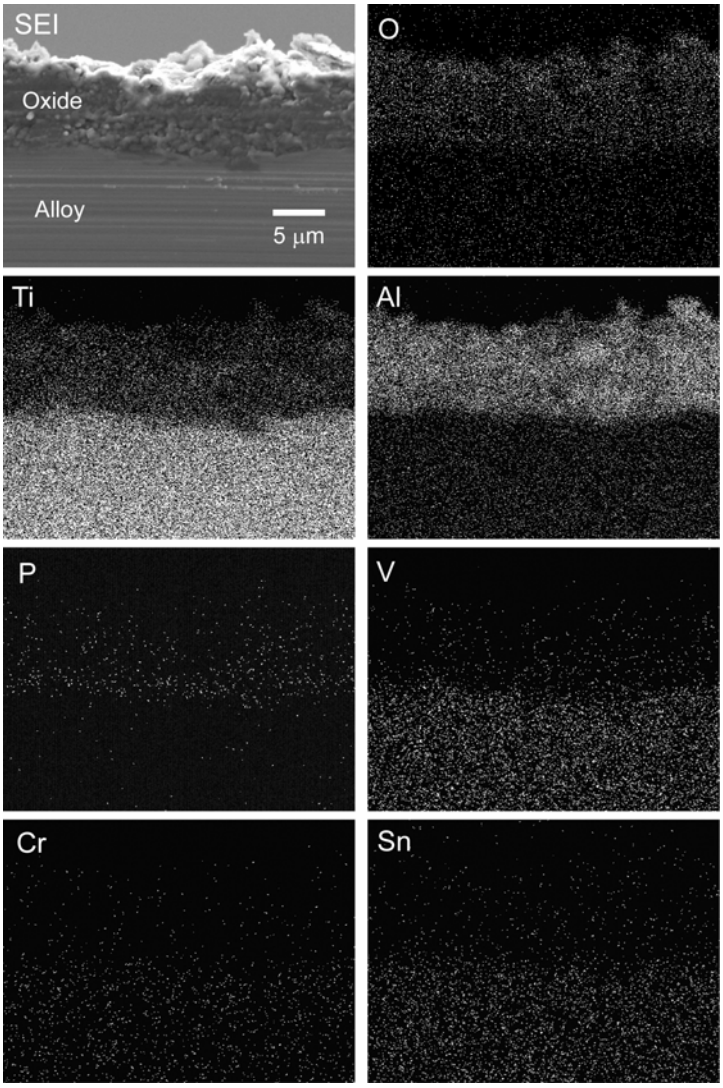

Fig. 7

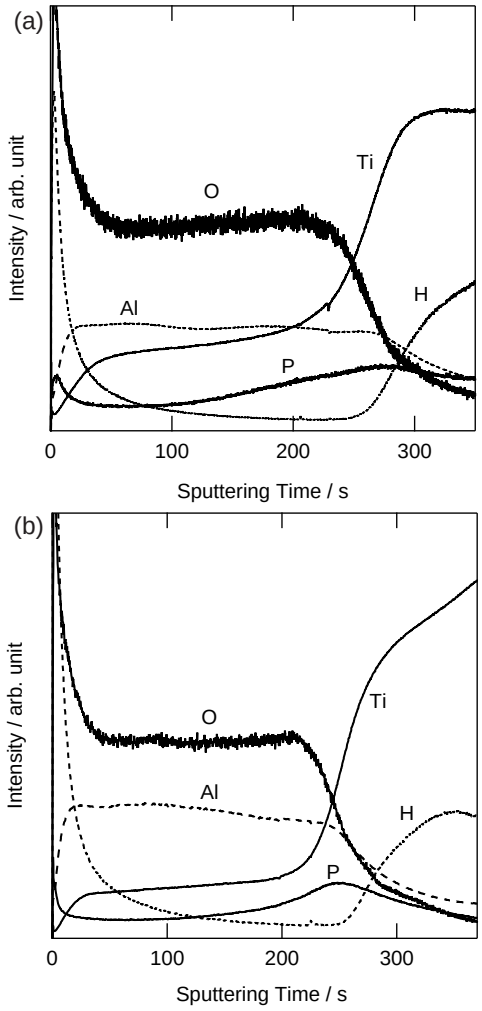
(a)
Intensity / arb. unit
O
Ti
Al
H
P
0
100
200
300
Sputtering Time / s
(b)
Intensity / arb. unit
O
Ti
Al
H
P
0
100
200
300
Sputtering Time / s

Fig. 8